

Effect of electron beam irradiation on thermally evaporated Ge₂Sb₂Te₅ thin films

D. SARKAR^a, G. SANJEEV^b, T. N. BHAT^{c,d}, M. G. MAHESHA^{a*}

^aDepartment of Physics, Manipal Institute of Technology, Manipal University, Manipal 576104, India

^bDepartment of Physics, Mangalore University, Mangalore 574119, India

^cInstitute of Materials Research and Engineering, A*STAR (Agency of Science, Technology, and Research), 117602 Singapore

^dDepartment of Materials Science, Mangalore University, Mangalore 574119, India

Ge₂Sb₂Te₅ (GST) thin films have been grown by thermal evaporation technique. The grown films have been irradiated with electron beam at various doses. As-deposited and irradiated films have been characterized for their structural, optical and electrical properties. Raman spectra has been recorded to get more insight on structural rearrangement that happened during the irradiation process. Detailed analysis of these data has been made to explore the behavior of system under electron irradiation environment.

(Received February 25, 2017; accepted February 12, 2018)

Keywords: GST, Phase change memory, Structural property, Optical property, Electrical property, Raman spectroscopy

1. Introduction

Phase change materials which exhibit phase transformation upon external irradiation or application of external voltage can be used to store digital information in their amorphous and crystalline phases. The absolute minimum quenching rate required for amorphization is different for various materials, ranging from 10⁶ to 10¹¹ K/s [1]. In optical route, medium power laser with typical spot size of 1 μm is used to irradiate the sample. Alternatively switching can be achieved by applied electric field also. Ge₂Sb₂Te₅ (GST) is the most commonly used phase change material in optical drives [2-8]. In recent years, exhaustive theoretical investigations have been made to understand the molecular dynamics of phase transition. Also attempts have been made by experimental techniques via extended x-ray absorption fine structure (XAFS) and Raman scattering measurements to comprehend the dynamics of phase transition in GST. These studies suggested that the structure of amorphous GST can be described as cross-section of a distorted rocksalt structure with vacancies and the amorphization of GST is due to an umbrella flip of Ge atoms from an octahedral position into a tetrahedral position [9]. Irradiation of semiconducting materials with energetic radiation can be adopted as a tool to introduce point defects in controlled mode and tailor the properties [10]. The induced defects can yield new electronic configurations which now have different coordination numbers than in the crystalline materials. Also radiation of suitable energy can enhance the number of intrinsic carriers (electrons and holes) by several orders of magnitude [11]. Additionally, these irradiation induced defects can result in vacancies and interstitials; in some

cases even defect clusters may also form [12]. With a view to get a better understanding of amorphous GST films irradiated by electron beam, we performed the investigations on a comprehensive morphology evolution and local fine microstructure of GST films by using Raman spectroscopy and atomic force microscopy (AFM). Raman spectroscopy have proven to be powerful and effective tools for characterizing the structure of local arrangements in glasses [13].

2. Experimental details

Amorphous GST films with a thickness of about 100 nm were deposited on glass substrates by thermal evaporation technique by maintaining the base pressure as 10⁻⁶ Torr. The substrate was maintained at room temperature and deposition rate was kept at 6 nm s⁻¹ by ramping the filament current. The X-ray diffraction (XRD) measurements are carried out with Cu Kα (1.54 Å) radiation using a Rigaku powder diffractometer with a scan speed of 2°/min. Energy dispersive x-ray spectroscopy (EDS) analysis is carried out using ZEISS EVO-18 system to determine the chemical composition of the prepared samples. The surface morphology of as-synthesized thermally evaporated GST films and the effect of electron beam irradiation on the morphology of films had been examined by using Bruker-Innova atomic force microscopy (AFM). The AFM images were analyzed using Nanoscope version 1.20 software. Optical transmittance and reflectance were recorded using Shimadzu UV-VIS-NIR spectrophotometer (model UV-3100). Raman spectra were collected in backscattering geometry using an Ar⁺ excitation source λ = 488 nm

coupled with a Labram-HR800 micro-Raman spectrometer equipped with a $\times 50$ objective, an appropriate notch filter, and a Peltier cooled charge coupled device detector. Sandwich geometry with aluminium (Al) as contact electrode was used for electrical study. In switching device fabrication, firstly, a thin layer of Al was deposited on a glass substrate which acts as a lower electrode (Fig. 1) and over that GST film was deposited with appropriate mask. Before the top electrode, the structure was exposed to electron beam irradiation at various doses at Microtron Center, Mangalore University, India with a peak energy of 8 MeV, beam current of 15–20 mA, pulse width of 1.5–2 ms at the dose rate of 0.017 kGy per second by maintaining the sample distance about 30cm. Resistance of as-deposited and irradiated films was estimated by four probe method.

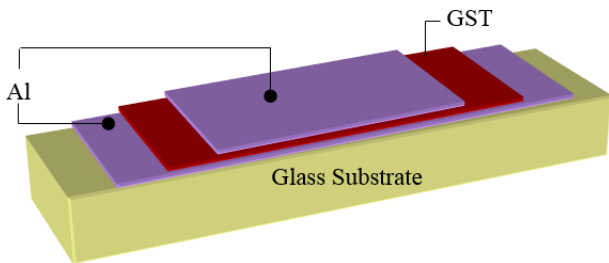


Fig. 1. Schematic representation of electrical switching device.

3. Results and discussion

3.1. Structural properties

X-ray diffractogram confirmed the amorphous nature of the as-deposited films. The broad diffuse pattern observed in the XRD pattern of as-deposited films confirmed the amorphous signature of the structural phases as shown in Fig. 2. No phase transition was observed after irradiation at various doses.

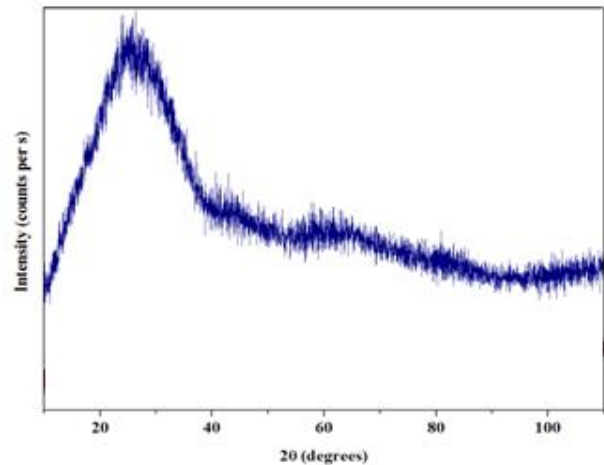


Fig. 2. XRD pattern of as-deposited GST thin films confirming amorphous nature

AFM micrographs reveal that the as-deposited GST thin films consisted of uniform and smaller grains. When the GST thin films irradiated with different electron doses, surface roughness has increased with dose initially and then started decreasing from 8kGy onwards. Exposure to radiations that excites electron-hole pairs produces structural changes in nearly all chalcogenide glasses and amorphous films. This results in changes in atomic configuration, and a subsequent change in the physical and chemical properties such as structure, optical and electronic transport properties of the materials [14]. Fig. 3 depicts the three-dimensional (3D) AFM images of GST film surface before and after irradiation. Morphological analysis of the irradiated amorphous GST films suggests that the structural changes in the deposits are associated with the tendency of the samples to undergo a certain local structural ordering on a microscopic scale, first of all, in the nearest neighbor environment of atoms. The as-grown GST films are found to be slightly Te-rich in composition as compared to that of the source material and no compositional change has been observed even after electron irradiation, as examined by electron dispersion spectroscopy (EDS). The surface morphology is an important aspect affecting the electrical and optical properties of devices irrespective of the growth procedure.

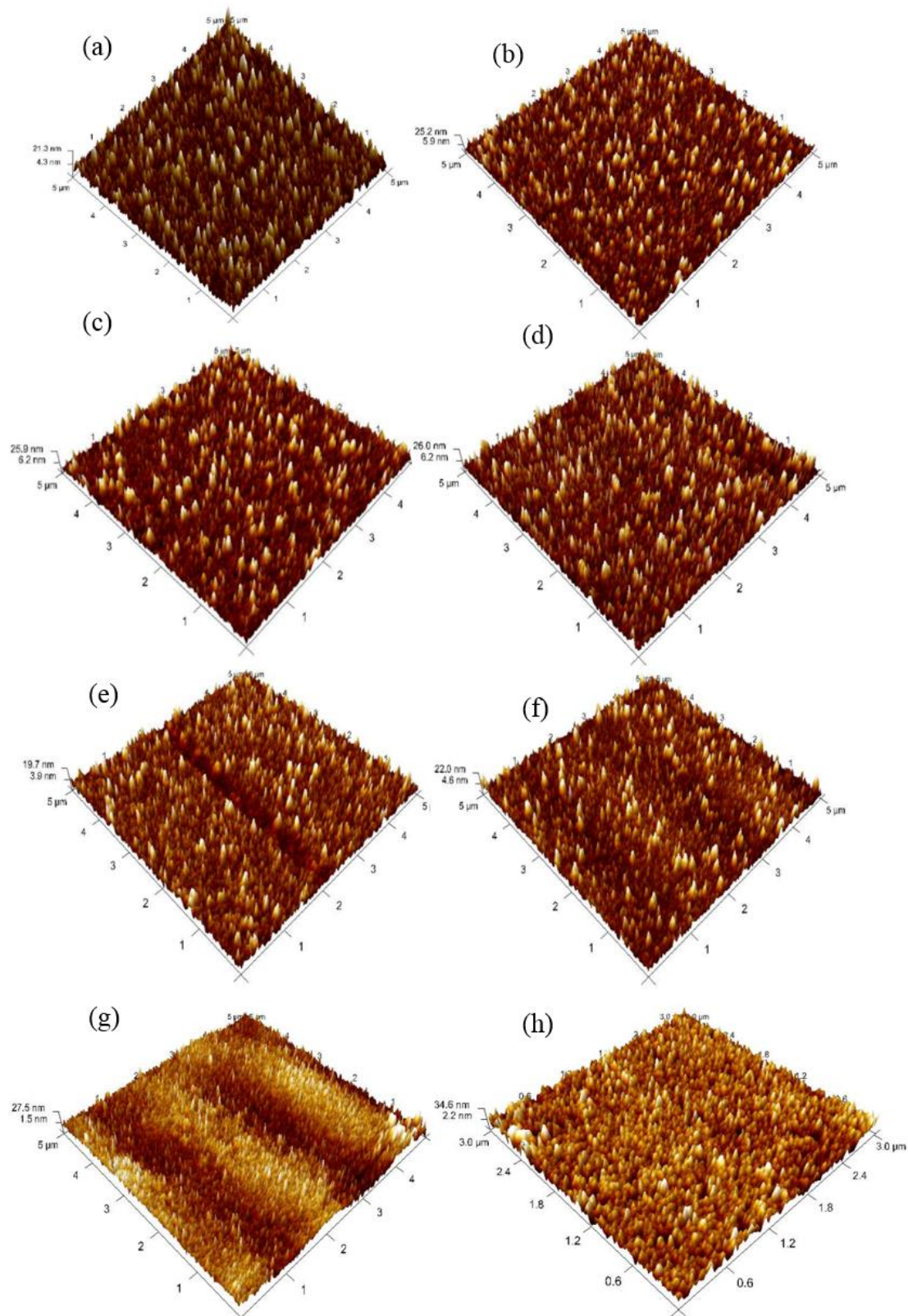


Fig. 3. AFM images (3D) of GST thin films irradiated with different doses (a) 0 kGy (b) 1 kGy (c) 2 kGy (d) 3 kGy (e) 4 kGy (f) 5 kGy (g) 6 kGy (h) 8 kGy respectively.

3.2. Optical properties

The optical band gap of GST thin films has been determined from the measured absorption spectra. The optical band gap of unirradiated and irradiated samples of

amorphous GST thin films had been calculated from absorption coefficient (α) data as a function of wavelength from the Tauc relation [9]:

$$\alpha h\nu = \text{const}(h\nu - E_g)^r$$

where the const. which is different for different transitions indicated by the different values of r and E_g is the corresponding band gap. The exponent r is an appropriate, selected index, which depends on the nature of electronic transition and is assumed to have a value of $1/2$ for direct transition and 2 for indirect transition, respectively. For the case of GST thin films, we choose $r = 2$ in the equation which corresponds to the optical transitions in most amorphous semiconductors as proposed by Tauc [15]. Many papers have shown $r = 2$ acceptable for amorphous chalcogenide semiconductors, including GST [16]. Fig. 4 shows a typical plot of $(\alpha h\nu)^2$ vs. $h\nu$ for the unirradiated GST thin films where energy band gap is obtained by intersecting the extrapolated line on the x-axis. The optical energy band gap (E_g) of unirradiated (0 kGy) GST thin film, obtained by intersecting the extrapolated line on the x-axis, is 0.71 eV. The E_g values reported in some other papers, approximately 0.7 eV for amorphous Ge₂Sb₂Te₅ thin films, were in good agreement with our own results [16]. The shift in the optical band gap of amorphous GST thin films after irradiation may be caused due to microstructural changes in the nearest neighbor environment of atoms and changes in the electron defect subsystem or may also be due to the strains that had been modified by electron irradiation possibly due to the elimination of defect accumulation.

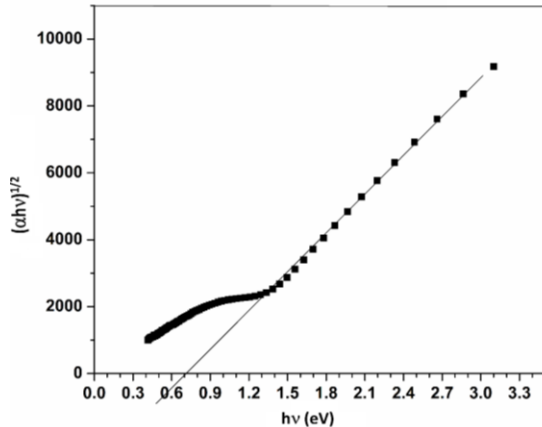


Fig. 4. Typical plots of $(\alpha h\nu)^2$ vs. $h\nu$ of GST (as deposited) thin films

Through the irradiation process, the strained or partially strained GST structures will be relaxed due to various processes for e.g. electronic excitation, heat generation etc. Since, electron beam would interact with amorphous GST differently for different grain sizes/boundaries as the ratio of surface to volume scattering changes. Also, as the sizes of particles begin to approach the wavelength of the electron beam involved, the fundamental scattering behavior will change. The increase in the optical band gap may be due to formation of grains, the reduction in the disorder and decrease in density of defect states (which results in the reduction of

tailing of bands). The transition in an amorphous semiconductor is called “direct” because it does not need phonon assistance. The direct transition in a crystal occurs between two states with the same k , whereas the transition in an amorphous semiconductor occurs without the k -space conservation rules [17].

3.3. Raman Spectroscopy

Raman spectra has been recorded for as-deposited and electron beam irradiated films and analyzed to get more insight on the irradiation induced structural modifications. The origin of the individual modes in GST films can be revealed by comparison with binary compounds in which the atoms are in the same local bonding geometry. Since the ternary GST material system is composed of the binary GeTe and Sb₂Te₃ compounds, the coherent phonon spectra of Ge₂Sb₂Te₅ and its binary constituents are compared to elucidate the origin of the modes observed. Since no long-range order exists in amorphous materials, only local phonon modes can be excited [18]. These points towards a similar short-range order in both amorphous Ge₂Sb₂Te₅ and amorphous GeTe. The observed Raman bands reflect some very basic structural features. Raman spectrum recorded for amorphous GST thin films exposed to different dose of electron irradiation is shown in Fig. 5. Total four Raman bands with various intensities have been identified in the Raman spectra in the range from 50-200 cm⁻¹. The observed, approximate Raman band positions in all the amorphous GST thin films irradiated with different electron doses are as follows: band A ~ 69.4, band B ~ 91.1, band C ~ 107.2 and band D ~ 150.0. Reasonable qualitative agreement has been found between the Raman bands observed in the present study and the bands previously reported for GeTe and GST compounds [19-22]. The mode analysis and main atomic motions involved are considered as given by Andrikopoulos *et al.* and Mazzarello. *et al.* [21-23]. According to Mazzarello *et al.*, the weak features in the range 60–80 cm⁻¹ correspond to the broad experimental peak at 75 cm⁻¹ (resolved in two Gaussian peaks at 65 and 88 cm⁻¹ and assigned to A1 vibrations of GeTe_{4-n} tetrahedral in Ref. [21]. The other main theoretical peak at 110 cm⁻¹ assigned to bending modes of corner sharing tetrahedral in Ref. [22]. An interesting feature that has been observed in Raman spectra is a remarkable change in the relative intensity of the vibrational modes with increasing electron dose. In Fig. 5, it is seen that large change is observed in the intensity of amorphous GST activated Raman modes as the irradiation doses is varied. Of the four distinguishable peaks observed in Raman spectra of pristine GST films, ~ 69.4 cm⁻¹ (A), ~ 91.1 cm⁻¹ (B), ~ 107.2 cm⁻¹ (C) are assigned to different vibrations of Ge-Te and ~ 150.0 cm⁻¹ (D) attributed to Sb-Te, respectively. Upon the detailed analysis of Raman spectra of amorphous GST thin films irradiated with different doses of electron irradiation, no frequency shift observed compared to as-deposited films. It is also interesting to note that, there occurs no vibration neither due to homopolar bonds nor Ge-Sb bonds.

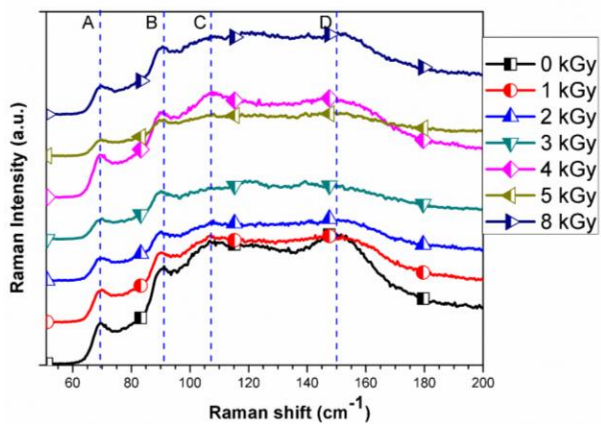


Fig. 5. Raman spectra of amorphous GST thin films irradiated with different doses.

3.4. Electrical properties

Electrical switching study has been performed on un-irradiated and irradiated GST thin films. Thermally evaporated GST thin films do not show smooth switching behavior as GeTe which has been presented in our earlier paper [24]. This may be due to the composition segregation during thermal evaporation, cluster formation or diffusion of elements into the electrode material or vis-a-versa. It indicates that thermal evaporation is not suitable for depositing multi component alloys. The failure of smooth switching behavior in GST devices could be due to the difference in mass density of the electrode material at the interface or due to electron irradiation induced void formation over the bottom electrode contact. The other main failure mechanism may possibly be elemental segregation, in particular Sb enrichment in the switching region caused by electro-migration. Instead of displaying switching phenomena, we represent resistance of different GST thin films irradiated with electron beam in Table 1. Here we observe a significant decrease in resistance, for 2kGy in accordance with higher and a reasonably lower value of surface roughness and band gap. The resistance further increased to 0.167 mΩcm for 3kGy, at the same time surface roughness also decreased to 5.39 nm whereas band gap increased to 0.71 eV. The results are consistent with the reported values [25]. These measurements could be correlated to each other either by band gap, surface roughness or the resistance values since they display a reasonably decrease or increase with respect to each other and seems inter dependent with electron irradiation.

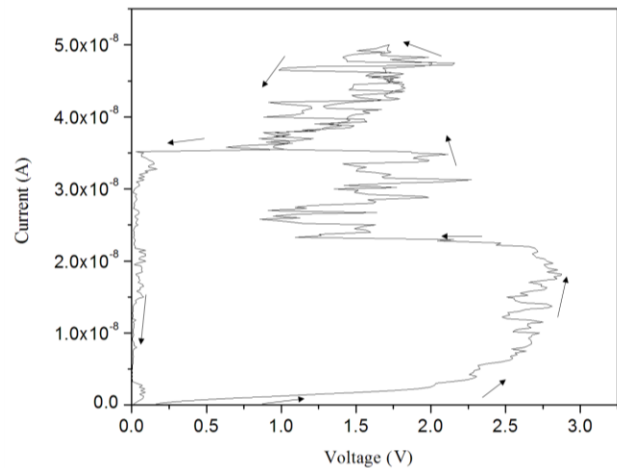


Fig. 6. Typical I-V plot showing poor electrical switching in GST thin films

Table 1. Comparison of band gap and resistivity of amorphous GST thin films as a function of electron doses

Dose	Band gap	Resistivity ($\times 10^{-3} \Omega\text{cm}$)
0	0.71	0.218
1	0.60	0.095
2	0.63	0.062
3	0.71	0.167
4	0.60	0.145
5	0.70	0.123
8	0.69	-

4. Conclusions

Effect of electron beam irradiation of thermally grown GST thin films has been studied in detail. AFM image analysis revealed that irradiation changes the surface roughness which could be due to local structural ordering in a microscopic scale. Change in the electrical resistance followed it. Also the change has been observed in optical band gap due to irradiation with a correlation between change in optical band gap and electrical resistance. Raman spectra analysis indicated the formation of Ge – Te bond and Sb – Te bond. Also interesting to note that neither homopolar bond nor Ge – Sb bond signatures were observed in Raman study.

Acknowledgements

The authors are thankful to Department of Atomic Energy, Board of Research in Nuclear Science, Mumbai (2011/34/17/BRNS/0586) India and VGST, Govt. of Karnataka (VGST/K-FIST(L1)/GRD-377/2014-15) for financial assistance.

References

- [1] Simone Raoux, Matthias Wuttig, Phase Change Materials Science and Applications, Springer Science Business Media (2009).
- [2] Jin Hwan Jeong, Jun Hyuk Park, Yeong Min Lee, Uk Hwang, Hyung Keun Kim, Deok Sin Kil, Doo Jin Choi, Materials Science in Semiconductor Processing **40**, 50 (2015).
- [3] J. H. Jeong, S. J. Park, S. B. An, D. J. Choi, J. Cryst. Growth **410**, 4 (2015).
- [4] A. Fantini, L. Perniola, M. Armand et al., Comparative assessment of GST and GeTe materials for application to embedded phase-change memory devices, Proceedings of IEEE International Memory Workshop (IMW), 2009.
- [5] F. Pellizzer, R. Bez, Phase-change memories for nano-scale technology and design, Proceedings of IEEE International Conference on IC Design and Technology (ICICDT), 2012, pp.1–4.
- [6] M. Zhu, M. Xia, F. Rao, X. Li, L. Wu, X. Ji, S. Lv, Z. Song, S. Feng, H. Sun, S. Zhang, Nat. Comm. **5**, 4086 (2014).
- [7] K. B. Borisenko, J. Shanmugam, B. A. O. Williams, P. Ewart, B. Gholipour, D. W. Hewak, R. Hussain, T. Javorfi, G. Siligardi, A. I. Kirkland, Scientific Rep. **5**, 8770 (2015).
- [8] D. Loke, J. M. Skelton, W.-J. Wang, T.-H. Lee, R. Zhao, T.-C. Chong, S. R. Elliott, PNAS **111**, 13272 (2014).
- [9] Alexander V. Kolobov, Paul Fons, Anatoly I. Frenkel, Alexei L. Ankudinov, Junji Tominaga and Tomoya Uruga, Nature Materials **3**, 703 (2004).
- [10] A. V. Krasheninnikov, K. Nordlund, J. Appl. Phys. **107**, 071301 (2010).
- [11] Zhou Dong, Wu Liangcai, Guo Qi, Peng Cheng, He Chengfa, Song Zhitang, Rao Feng, Li Yudong, Xi Shanbin, Journal of Alloys and Compounds **575**, 229 (2013).
- [12] J. J. Zhao, F. R. Liu, X. X. Han, N. Bai, Y. H. Wan, X. Lin, F. Liu, Applied Surface Science **289**, 160 (2014).
- [13] S. Y. Kim, H. S. Lee, I. S. Chung, Y. J. Park, J. Y. Lee, T. W. Kim, Applied Surface Science **253**, 4041 (2007).
- [14] S. Subramanian, M. Balaji, P. Chithra lekha, Ganesh Sanjeev, E. Subramanian, D. Pathinettam Padiyan, Radiation Physics and Chemistry **79**, 1127 (2010).
- [15] J. Tauc, Amorphous and Liquid Semiconductors, Plenum publishing company, 1974
- [16] B. S. Lee, J. R. Abelson, S. G. Bishop, D-H Kang, B-K Cheong, K-B Kim, J. Appl. Phys. **97**, 093509 (2005).
- [17] Bong-Sub Lee, John R. Abelson, Stephen G. Bishop, Dae-Hwan Kang, Byung-ki Cheong Ki-Bum Kim, Journal of Applied Physics **97**, 093509 (2005).
- [18] M. Forst, T. Dekorsy, C. Trappe, M. Laurenzis, H. Kurz, Applied Physics Letters **77**, 1964 (2000).
- [19] E. M. Vinod, K. S. Sangunni, Thin Solid Films **550**, 569 (2014).
- [20] Fu Jing, Shen Xiang, Nie Qihua, Wang Guoxiang, Wu Liangcai, Dai Shixun, Xu Tiefeng, R. P. Wang, Applied Surface Science **264**, 269 (2013).
- [21] K. S. Andrikopoulos, S. N. Yannopoulos, A. V. Kolobov, P. Fons, J. Tominaga, J. Phys. Chem. Solids **68**, 1074 (2007).
- [22] K. S. Andrikopoulos, S. N. Yannopoulos, G. A. Voyiatzis, A. V. Kolobov, M. Ribes, J. Tominaga, J. Phys.: Condens. Matter **18**, 965 (2006).
- [23] R. Mazzarello, S. Caravati, S. A. Uberti, M. Bernasconi, M. Parrinello, Phys. Rev. Lett. **104**, 085503 (2010).
- [24] Deepangkar Sarkar, Ganesh Sanjeev, M. G. Mahesha, Applied Physics A **119**, 49 (2015).
- [25] K. Cil, F. Dirisaglik, L. Adnane, M. Wennberg, A. King, A. Farclas, M. B. Akbulut, A. Gokirmak, H. Silva, Y. Zhu, C. Lam, IEEE Trans. Electron Dev. **60**, 433 (2013).

*Corresponding author: maheshamg@gmail.com